Journal Pre-proof

Synthesis, lattice energy and microwave dielectric properties of $BaCu_{2-x}Co_xSi_2O_7$ ceramics

Xiao-Qiang Song, Wen-Zhong Lu, Yi-Hui Lou, Tao Chen, Shi-Wo Ta, Zhen-Xiao Fu, Wen Lei

PII: S0955-2219(20)30156-4

DOI: https://doi.org/10.1016/j.jeurceramsoc.2020.02.048

Reference: JECS 13095

To appear in: *Journal of the European Ceramic Society*

Received Date: 18 October 2019

Revised Date: 21 February 2020

Accepted Date: 21 February 2020

Please cite this article as: Song X-Qiang, Lu W-Zhong, Lou Y-Hui, Chen T, Ta S-Wo, Fu Z-Xiao, Lei W, Synthesis, lattice energy and microwave dielectric properties of $BaCu_{2-x}Co_xSi_2O_7$ ceramics, *Journal of the European Ceramic Society* (2020), doi: https://doi.org/10.1016/j.jeurceramsoc.2020.02.048

Synthesis, lattice energy and microwave dielectric properties of $BaCu_{2-x}Co_xSi_2O_7$ ceramics

Xiao-Qiang Song[a,b], Wen-Zhong Lu[a,b], Yi-Hui Lou[a,b], Tao Chen[c], Shi-Wo Ta[c*], Zhen-Xiao Fu[c], Wen Lei[a,b*]

[a] School of Optical and Electronic Information, Huazhong University of Science and Technology, Wuhan 430074, P. R. China

[b] Key Lab of Functional Materials for Electronic Information (B), Ministry of Education, Wuhan 430074, P. R. China

[c] State Key Laboratory of Advanced Materials and Electronic Components, Guangdong Fenghua Advanced Technology Holding Co., Ltd., Zhaoqing 526020, P. R. China

[*] Corresponding author. Tel.: +86 27 8755 6493; fax: +86 27 8754 3134.
E-mail address: wenlei@mail.hust.edu.cn (W. Lei) and tashiwo@china-fenghua.com (S.W. Ta)

Abstract

$BaCu_{2-x}Co_xSi_2O_7$ solid solutions with orthorhombic structure (Pnma) were prepared by solid-state reaction method. The phase synthesis process, structural evolution and microwave dielectric properties of $BaCu_{2-x}Co_xSi_2O_7$ ceramics were investigated. Single $BaCu_2Si_2O_7$ phase was obtained when calcined at 950 ºC for 3 h and was decomposed into $BaCuSi_2O_6$ phase when calcined at 1075 ºC for 3 h. The sintering process was effectively promoted when Cu^{2+} was replaced by Co^{2+} and the maximum solubility of $BaCu_{2-x}Co_xSi_2O_7$ was located between 0.15 and 0.20. P-V-L complex chemical bond theory and Raman spectra were used to explain the structure-property correlations of $BaCu_{2-x}Co_xSi_2O_7$ ceramics. The corrected dielectric constant ($\varepsilon_{r\text{-}corr}$) of $BaCu_{2-x}Co_xSi_2O_7$ ceramics decreased monotonously with the susceptibility ($\Sigma\chi^{\mu}$) and ionic polarizability of primitive unit cell. The quality factor ($Q\times f$) increased with bond strength and lattice energy (U_{cal}), especially the lattice energy of the Si-O bond. The temperature coefficient of resonant frequency (τ_f) was determined by the susceptibility and lattice energy of the Cu/Co-O bond. The following optimum microwave dielectric properties were obtained at $x = 0.15$ when sintered at 1000 ºC for 3 h: $\varepsilon_r = 8.45$, $Q\times f =$ 58958 GHz and $\tau_f = -34.4$ ppm/ºC.

Key words: microwave dielectric properties; melilite; $BaCu_2Si_2O_7$

1. Introduction

Microwave dielectric ceramics are used in dielectric resonators, filters and substrates etc. [1]. For 5G wireless communication systems, a high frequency, a low latency, a low-loss of the electronic devices and miniaturization are required; the number of electronic devices has increased dramatically due to the high transmission speed and short transmission distance of 5G signal [2]. Microwave dielectric ceramics with low dielectric constant, high quality factor and near-zero temperature coefficient of resonant frequency are needed for 5G wireless communication to achieve high signal transmission speed, good signal selectivity and excellent temperature stability [3]. Therefore, a number of microwave dielectric ceramics with low dielectric constant have been investigated [4-6].

Melilite-type silicates and germinates exhibit a variety of novel properties, such as ferroelectricity, ferromagnetic and negative thermal expansion [7-9]. Two different melilite-type compounds, namely, $A_2BC_2O_7$ and $AB_2C_2O_7$ (A = Ca, Sr, Ba; B = Mg, Zn, Co, Ni, Mn, Cu and C = Si, Ge), are determined by the relative amount of A-site and B-site ions. Sebastian et al. [10] systematically investigated the microwave dielectric properties of $(Sr_{1-x}A)_2(Zn_{1-x}B_x)Si_2O_7$ ceramics (A = Ca, Ba and B = Mg, Co, Ni, Mn). A phase transition from tetragonal to monoclinic was observed in $(Sr_{1-x}Ba_x)_2ZnSi_2O_7$ solid solutions, and the optimum microwave dielectric properties were obtained for $Sr_2ZnSi_2O_7$ (ε_r = 8.40, $Q\times f$ = 105000 GHz and τ_f = -51.5 ppm/°C). Xiao et al. [11,12] revealed the correlations between the crystal structure and microwave dielectric properties of $A_2MgSi_2O_7$ ceramics (A = Ca, Sr) by using complex chemical bond theory. Li et al. [13] reported the microwave dielectric properties of $Ba_2MgGe_2O_7$ and $Ba_2ZnGe_2O_7$ ceramics, which show a tetragonal melilite-type structure. Thus far, much attention has been paid to $A_2BC_2O_7$ type melilite microwave dielectric ceramics, but the microwave dielectric properties of $AB_2C_2O_7$ type melilite ceramics have been rarely studied. In previous work, we investigated the relationships among the crystal structure, lattice energy and microwave dielectric properties of $BaCo_2Si_2O_7$ ceramic and found that it presents good microwave dielectric properties (ε_r = 9.26, $Q\times f$ = 31135 GHz and τ_f = -92.1 ppm/°C). The difference in the crystal structure between $A_2BC_2O_7$ and $AB_2C_2O_7$ is the connection method between $[BO_4]^{2-}$ and $[C_2O_7]^{6-}$. The $[C_2O_7]^{6-}$ group and $[BO_4]^{2-}$ tetrahedra in $A_2BC_2O_7$ connects each other in the a-c plane; therefore,

$A_2BC_2O_7$ shows a layered structure, and A^{2+} is located between the two layers. For $AB_2C_2O_7$, $[BO_4]^{2-}$ tetrahedra connect with one another in the *a-c* plane and form a $[BO_4]^{2-}$ chain. The $[BO_4]^{2-}$ chain in the *a-c* plane connects with the $[C_2O_7]^{6-}$ group in the *a-b* plane and forms a skeleton structure. Finally, the polyhedral gap is filled by A^{2+}. $[CuO_4]^{2-}$ is not a tetrahedral but a rectangular plane in $BaCu_2Si_2O_7$ due to the particularity of the extranuclear electron distribution of Cu. $BaCu_2Si_2O_7$ has become a research hotspot in ferromagnetism because of its interesting crystal structure [14], but its dielectric properties has not been reported yet.

In this work, melilite-type $BaCu_{2-x}Co_xSi_2O_7$ ceramics were prepared and characterized. Phase synthesis process was characterized by the differential scanning calorimetry analysis (DSC) and thermogravimetry (TG). Lattice energy, bond susceptibility and linear thermal expansion coefficient were calculated based on the complex chemical bond theory. The relationships among microstructure, crystal structure, lattice energy and microwave dielectric properties of $BaCu_{2-x}Co_xSi_2O_7$ ceramics were also systematically investigated for the first time.

2. Experimental procedure

$BaCu_{2-x}Co_xSi_2O_7$ ceramics were prepared by the conventional solid-state method using reagent grade $BaCO_3$ (99.8%), CuO (99.8%), CoO (99.9%) and SiO_2 (99.5%) powders as raw materials. Based on the chemical formula, the raw materials were weighed and ball milled in a polyethylene jar for 5 h using ZrO_2 balls with deionized water. After drying at a temperature of 90 °C, the mixtures were calcined in air at 900 °C-1075 °C for 3 h with a heat rate of 5 °C/min. Then, the powders were uniaxially pressed into samples with dimensions of 12 mm in diameter and approximately 6 mm in height under a pressure of 150 MPa. The samples were sintered in a temperature range of 975 °C-1050 °C for 3 h with a heating rate of 5 °C/min, and then they were naturally cooled in the furnace. The relative density ρ_{rel} was calculated by:

$$\rho_{rel} = \frac{\rho_{bul}}{\rho_{the}} \qquad (1)$$

where ρ_{bul} is the bulk density that measured by Archimedes' method and ρ_{the} is the theoretical density.

The XRD data were obtained using X-ray diffraction (XRD, XRD-7000, Shimadzu, Kyoto, Japan) with CuKα radiation. The phase analysis was performed by Rietveld refinement using GSAS and EXPGUI software [15-17]. The microstructure of the $BaCu_{2-x}Co_xSi_2O_7$ samples were measured using a scanning electron microscope (SEM, Sirion 200, Netherlands). The DSC and TG were carried out on a STA449F3 thermal analysis instrument with a heating rate of 10 ºC/min. Raman measurements were performed at room temperature by HR-800 Lab Raman. The 532 nm line of the Nd: YAG laser beam was focused with an output of 50 mW on the sample. The ε_r and the unloaded $Q\times f$ value was measured in the microwave frequency range (12-14 GHz) in the TE_{011} mode by parallel plate cavity method [18] using a vector network analyzer (Agilent E8362B, Agilent Technologies, USA) and parallel silver boards. The τ_f value in the temperature range of 30 °C to 80 °C was calculated by Eq. (2):

$$\tau_f = \frac{1}{f(T_0)} \frac{[f(T_1) - f(T_0)]}{T_1 - T_0} \qquad (2)$$

where $f(T_1)$ and $f(T_0)$ represent the resonant frequency at T_1 (80 °C) and T_0 (30 °C), respectively.

3. Results and discussion

3.1 Synthesis and phase characterization

Fig. 1(a) shows the DSC/TG curve of the $BaCO_3$-2CuO-$2SiO_2$ mixture. Region M1 corresponds to the decomposition process of $BaCO_3$ and can be represented by Eq. (S1) in supplementary file. The decomposition product BaO reacts with SiO_2 to form $BaSiO_3$ phase, and an exothermic stage appears in M2 (Eq. (S2)). Region M3 is the synthesis process of $BaCu_2Si_2O_7$ (Eq. (S3) and (S4)), and this process differs from the phase-formation process of $BaCuSi_2O_6$ [19]. A weak endothermic peak appears in region M4 due to the reduction process of Cu^{2+} into Cu^+ in $BaCu_2Si_2O_7$ (Eq. (S5)). Finally, a strong endothermic peak appears in M5, and loss of weight is found in the TG curve, indicating that $BaCu_2Si_2O_7$ begins to break down (Eq. (S6)). X-ray powder diffraction (XRD) patterns of $BaCO_3$-2CuO-$2SiO_2$ mixture calcined at different temperatures are shown in Fig. 1(b). The $BaCu_2Si_2O_7$ phase increases with increasing calcining temperature, and pure $BaCu_2Si_2O_7$ is obtained when calcined at 950 ºC-1050

ºC. However, $BaCu_2Si_2O_7$ is decomposed into $BaCuSi_2O_6$ when calcined at 1075 ºC. Therefore, 950 ºC was selected as the calcining temperature for $BaCO_3$-2CuO/CoO-$2SiO_2$.

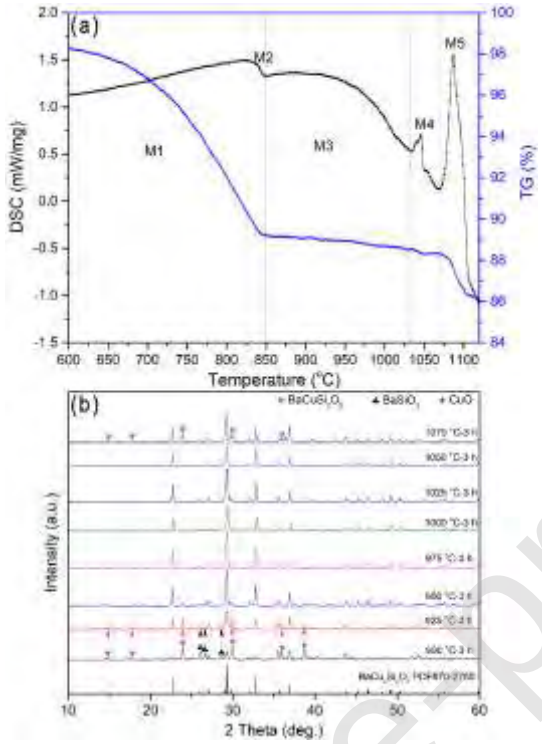

Fig. 1 (a) DSC-TG curves of $BaCO_3$-2CuO-$2SiO_2$ mixture and (b) XRD patterns of $BaCu_2Si_2O_7$ calcined at different temperatures.

3.2 Structural evolution of $BaCu_{2-x}Co_xSi_2O_7$ solid solutions

Fig. 2 shows the XRD patterns of $BaCu_{2-x}Co_xSi_2O_7$ ceramics prepared at the optimum sintering temperature. Single $BaCu_2Si_2O_7$ phase with an orthorhombic structure (Pnma) is obtained for x = 0-0.15; however, second phase SiO_2 is indexed for x = 0.20. The maximum solubility of $BaCu_{2-x}Co_xSi_2O_7$ is located within 0.15-0.20. Rietveld refinement is performed using $BaCu_2Si_2O_7$ (Pnma) as the initial structure model to analyze the crystal structural evolution of $BaCu_{2-x}Co_xSi_2O_7$ (Fig. S1). The example of the refined structural parameters from XRD data for $BaCu_{2-x}Co_xSi_2O_7$ (x = 0.15) is also listed in Table S1.

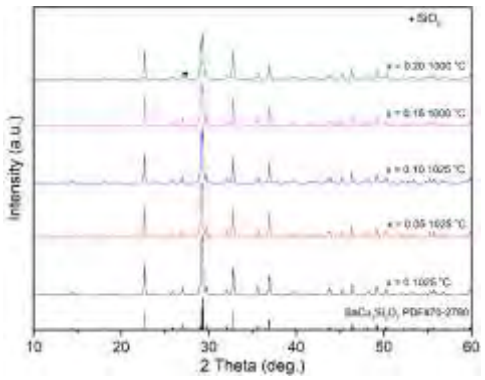

Fig. 2 XRD patterns of $BaCu_{2-x}Co_xSi_2O_7$ ceramics sintered at the optimum temperatures.

Cell parameters *b*, *c* and *V* in Table 1 and Fig. 3(a) increase linearly with the *x* value due to the larger ionic radius of Co^{2+} (CN = 4, $r(Co^{2+})$ = 0.58 Å) than that of Cu^{2+} (CN = 4, $r(Cu^{2+})$ = 0.57 Å) [20]. Cell parameter *a* decreases monotonously with the increasing of Co^{2+} content, and this interesting phenomenon is associated with the average bond length and connection method of the $[Cu/CoO_4]^{2-}$ plane. The variation in the average bond length of Cu/Co-O is shown in Fig. 3(b). The average bond length of Cu/Co-O bond increases with the *x* value, but the average bond length of Ba-O and Si-O bonds decreases linearly.

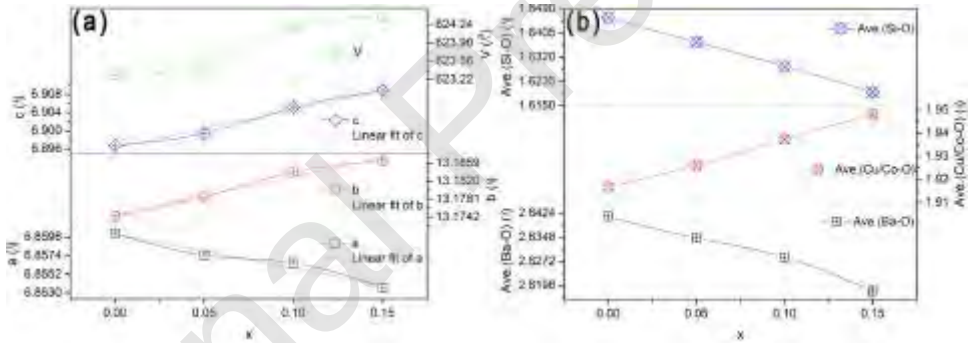

Fig. 3 (a) Lattice parameters of $BaCu_{2-x}Co_xSi_2O_7$ (x = 0-0.15) and (b) average bond length of Ba-O bond, Cu-O bond and Si-O bond.

Fig. S2 shows the crystal structure of $BaCu_2Si_2O_7$ (2×2×2). The $[Cu/CoO_4]^{2-}$ chains present a zigzag shape along the *c* axis (Fig. S2 (c)). The chain will stretch along the *c* axis and the bending of the $[Cu/CoO_4]^{2-}$ chain along *a* axis will reduce when the average bond length of Cu/Co-O bond increases. These changes will increase cell parameter *c* and decrease the cell parameter *a*. It is a very common phenomenon for the cell parameters to exhibit anisotropy trend as a function of the composition and temperature in $AB_2C_2O_7$-type melilite, which may lead to a negative or near-zero

thermal expansion coefficient [21]. The linear fit of the cell parameters *a*, *b*, and *c* are presented in Fig. 3(a), and the slopes of the fitted curve for *a*, *b*, and *c* are -0.040, 0.082 and 0.084, respectively. Each direction in the unit cell has two columns of Cu/Co atoms; thus, the normalized slopes for *a*, *b*, and *c* are -0.020, 0.041 and 0.042, respectively. The normalized slope for *c* is larger than *b* because of the stretching of $[Cu/CoO_4]^{2-}$ chains along the *c* axis.

Fig. 4(a) shows the Raman spectra of $BaCu_{2-x}Co_xSi_2O_7$ (x = 0-0.15) measured at room temperature. The observed Raman modes of the $BaCu_2Si_2O_7$ sample and the tentative assignment of major Raman bands from references [22,23] are listed in Table S2. In generally, the Raman spectra of $BaCu_{2-x}Co_xSi_2O_7$ can be divided into four regions. Region 1, < 420 cm^{-1}, is associated with the rotational and translational modes of $[SiO_4]$ tetrahedra and the Ba-O and Cu-O stretch modes. Region 2, between 420 cm^{-1} and 660 cm^{-1}, is ascribed to the O-Si-O symmetric and anti-symmetric bending vibrations (ν_2 and ν_4 modes) in $[SiO_4]$ tetrahedra. Region 3, ranging from 660 cm^{-1} to 700 cm^{-1}, is associated with the Si-O-Si bending vibrations within the $[Si_2O_7]^{6-}$ group. Region 4, between 800 cm^{-1} and 1100 cm^{-1}, is ascribed to the Si-O symmetric and anti-symmetric stretching vibrations (ν_1 and ν_3 modes) within the $[SiO_4]$ tetrahedra [22]. The Raman shift of the 160 cm^{-1}, 275 cm^{-1}, 898 cm^{-1} bands and the full width at half maximum (FWHM) of ν_1 mode at 898 cm^{-1} are shown in Fig. 4(b). The Raman shift of the band at 275 cm^{-1} (Cu-O stretch) decreases with the increasing of x value, whereas, the Raman shift of the bands at 160 cm^{-1} (Ba-O stretch) and 898 cm^{-1} ($[SiO_4]$ symmetric stretching) presents an opposite trend. A close correlation exists between the Raman shift and bond strength [24], and the variation in the Raman shift shows an opposite trend with the average bond length in Fig. 3(b). The stretching frequency of the chemical bond is inversely proportional to the bond length. The bond strength of Si-O increases and the damping behaviour decreases with decreasing average bond length of Si-O. Therefore, the FWHM of ν_1 mode at 898 cm^{-1} increases inversely in Fig. 4(b) [25-28].

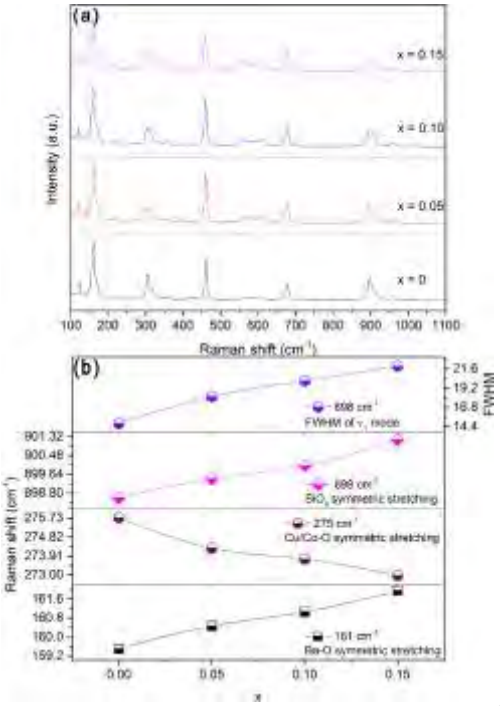

Fig. 4 (a) Raman spectra of $BaCu_{2-x}Co_xSi_2O_7$ (x = 0-0.15), (b) Raman shift of the 160 cm^{-1} band (Ba-O stretch), 275 cm^{-1} band (Cu/Co-O stretch) and 898 cm^{-1} band ([SiO_4] symmetric stretching) and FWHM of v_1 mode at 898 cm^{-1}.

Fig. S3 shows the micrographs of thermally etched $BaCu_{2-x}Co_xSi_2O_7$ ceramics sintered at the optimum temperature. Some large pores can be observed on the thermally etched surface for x = 0, and the number of pores decreases dramatically when the x value increases from 0 to 0.15. The grain size increases slightly and distribution of the grain size becomes more uniform with increasing the Co^{2+} content. The increasing relative density (Table 1) and the reducing optimum sintering temperature indicate that the doping of Co^{2+} can promote the sinterability of $BaCu_2Si_2O_7$ ceramics.

3.3 Lattice energy and microwave dielectric properties of $BaCu_{2-x}Co_xSi_2O_7$ solid solutions

Table 2 shows the microwave dielectric properties of $BaCu_{2-x}Co_xSi_2O_7$ ceramics sintered at the optimum temperature. Microwave dielectric properties are determined by the intrinsic factors and extrinsic factors. Extrinsic factors include the pores, second phase and grain boundary etc. [29,30]. In this work, $BaCu_{2-x}Co_xSi_2O_7$ (x = 0-0.15) ceramics are the pure $BaCu_2Si_2O_7$ phase and present high relative density (> 95%). Therefore, the microwave dielectric properties of $BaCu_{2-x}Co_xSi_2O_7$ ceramics are mainly

determined by intrinsic factors, and the effects of extrinsic factors will not be discussed in detail. Phillips-Van Vechten-Levine (P-V-L) theory is an effective method to reveal the relationships between the crystal structure and microwave dielectric properties [31-36]. Bond susceptibility χ^{μ}, lattice energy and linear thermal expansion coefficient can be calculated based on the P-V-L theory; these parameters are highly correlated with the microwave dielectric properties.

The complex crystal of $BaCu_2Si_2O_7$ should be decomposed into binary crystals according to the P-V-L theory before calculating the susceptibility χ^{μ} and lattice energy, and the chemical formula is written as follows [37]:

$BaCu_2Si_2O_7 = BaCu_2Si_2O(1)O(2)_2O(3)_2O(4)_2 = Ba_{1/7}O(1)_{1/3} + Ba_{2/7}O(2)^1{}_{1/2} + Ba_{2/7}O(2)^2{}_{1/2} + Ba_{2/7}O(3)_{2/3} + Cu_{1/2}O(2)_{1/2} + Cu_{1/2}O(3)_{2/3} + Cu_{1/2}O(4)^1{}_{2/3} + Cu_{1/2}O(4)^2{}_{2/3} + Si_{1/2}O(1)_{2/3} + Si_{1/2}O(2)_{1/2} + Si_{1/2}O(3)_{2/3} + Si_{1/2}O(4)_{2/3}$

For microwave dielectric ceramics, the polarization is determined by the electron displacement polarization and ionic displacement polarization. Based on P-V-L theory, dielectric constant can be expressed by susceptibility χ^{μ} as follows [36,38,39]:

$$\varepsilon = \sum_{\mu} \varepsilon^{\mu} \quad (3)$$

$$\varepsilon^{\mu} = 1 + 4\pi\chi^{\mu} \quad (4)$$

$$\chi^{\mu} = \frac{\left(\hbar\Omega_p^{\mu}\right)^2}{4\pi\left(E_g^{\mu}\right)^2} \quad (5)$$

where $\Omega_p{}^{\mu}$ is the plasma frequency of the μ bond, and $E^{\mu}{}_g$ is the average energy gap of μ bond. Aside from P-V-L method, dielectric constant can also be predicted by the Clausius-Mossotti (C-M) equation [40]:

$$\varepsilon_{r-cal} = \frac{3V_m + 8\pi\alpha_D^T}{3V_m - 4\pi\alpha_D^T} \quad (6)$$

$$\alpha_D^T = \alpha\left(Ba^{2+}\right) + (2-x)\alpha\left(Cu^{2+}\right) + x\alpha\left(Co^{2+}\right) + 2\alpha\left(Si^{4+}\right) + 7\alpha\left(O^{2-}\right) \quad (7)$$

where $\alpha(Ba^{2+})$, $\alpha(Cu^{2+})$, $\alpha(Co^{2+})$, $\alpha(Si^{4+})$ and $\alpha(O^{2-})$ are the ionic polarizability of Ba^{2+}, Cu^{2+}, Co^{2+}, Si^{4+} and O^{2-}, respectively; V_m is the primitive unit cell volume. The measured dielectric constant (ε_r or $\varepsilon_{r\text{-}mea}$) is corrected to further eliminate the effect of pores on the dielectric constant as follows [41]:

$$\varepsilon_{r-corr} = \varepsilon_{r-mea}\left[1+1.5(1-\rho_{rel})\right] \quad (8)$$

where $\varepsilon_{r\text{-}corr}$ is the corrected dielectric constant, and ρ_{rel} is the relative density.

Fig. 5(a) and Table S3 show the bond susceptibility χ^{μ} of $BaCu_{2-x}Co_xSi_2O_7$ ceramics. The susceptibility χ^{μ} of Cu/Co-O bond increases monotonously from $x = 0$ to $x = 0.15$, but the susceptibility χ^{μ} of Ba-O and Si-O bonds shows a decreasing trend. Interestingly, the variation in bond susceptibility χ^{μ} exhibits the same trend with the average bond length in Fig. 3(b). Short bond length, that is, strong bond strength, weakens ionic displacement polarization; hence, bond susceptibility χ^{μ} will decrease. This phenomenon can also be explained by the Raman shift in Fig. 4(b). Usually, a high wave number corresponds to high vibration energy, leading to a low dielectric constant [24,42]. Although the total bond susceptibility ($\Sigma\chi^{\mu}$) decreases with the x value, the measured dielectric constant (ε_r or $\varepsilon_{r\text{-}mea}$) increases. Thus, the measured dielectric constant should be corrected to eliminate the effect of pores. Fig. 5(b) shows the ionic polarizability of the primitive unit cell (α_D^T /Vm) and dielectric constant of $BaCu_{2-x}Co_xSi_2O_7$. The corrected dielectric constant ($\varepsilon_{r\text{-}corr}$) decreases with the increasing of the x value. This trend is the same with that of ionic polarizability of primitive unit cell (α_D^T /V_m) and the calculated dielectric constant ($\varepsilon_{r\text{-}cal}$). Thus, the measured dielectric constant (ε_r or $\varepsilon_{r\text{-}mea}$) is dominated by the ionic polarizability and pores (relative density).

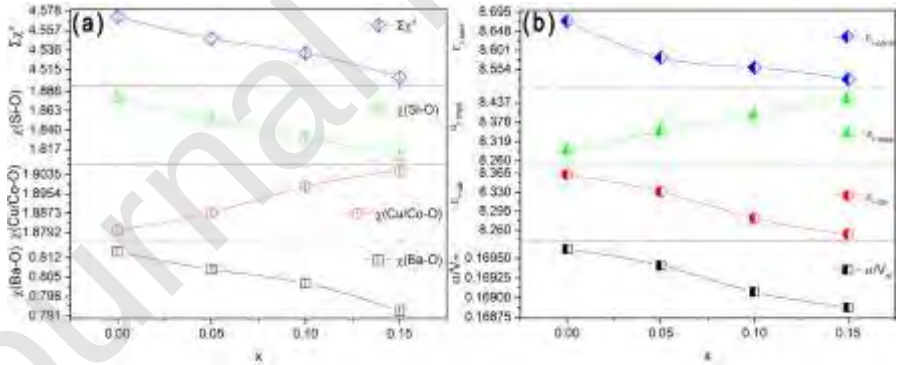

Fig. 5 (a) Bond susceptibility χ^{μ} of $BaCu_{2-x}Co_xSi_2O_7$ ceramics and (b) ionic polarizability of primitive unit cell (α_D^T /Vm) and dielectric constant of $BaCu_{2-x}Co_xSi_2O_7$.

Quality factor represents the dielectric loss of ceramics and is related to the crystal structure, packing fraction and lattice energy etc. [43,44]. Total lattice energy (U_{cal}) can be calculated using the following equations [45]:

$$U_{cal} = \sum_{\mu} \left(U_{bc}^{\mu} + U_{bi}^{\mu} \right) \quad (9)$$

$$U_{bc}^{\mu} = 2100 m^{\mu} \frac{\left(Z_{+}^{\mu} \right)^{1.64}}{\left(d^{\mu} \right)^{0.75}} f_{c}^{\mu} \quad (10)$$

$$U_{bi}^{\mu} = 1270 \frac{\left(m^{\mu} + n^{\mu} \right) Z_{+}^{\mu} Z_{-}^{\mu}}{d^{\mu}} \left(1 - \frac{0.4}{d^{\mu}} \right) f_{i}^{\mu} \quad (11)$$

where U_{bi}^{μ} and U_{bc}^{μ} are the lattice energy of the ionic and covalent parts of the μ bond, respectively; Z_{+}^{μ} and Z_{-}^{μ} are the valence states of cations and anions in μ bond, respectively; and f_{i}^{μ} and f_{c}^{μ} are the bond ionicity and covalency of the μ bond, respectively.

Fig. 6(a) shows the $Q \times f$ value and total lattice energy of Ba-O, Cu/Co-O, Si-O bonds and $BaCu_{2-x}Co_xSi_2O_7$. The quality factor increases linearly and reaches the maximum value at $x = 0.15$. This trend is the same with that of the lattice energy of Ba-O bond (ΣU(Ba-O)), Si-O bond (ΣU(Si-O)) and the total lattice energy of $BaCu_{2-x}Co_xSi_2O_7$ (U_{cal}). The percentage of lattice energy for each chemical bond to the U_{cal} is approximately 5.84% for Ba-O bond, 18.75% for Cu/Co-O bond and 75.41% for Si-O bond. The lattice energy U_{cal} is mainly contributed by the Si-O bond, which indicates that the $Q \times f$ value of $BaCu_{2-x}Co_xSi_2O_7$ ceramics is dominated by the lattice energy of Si-O bond. Based on the analysis of the the Raman spectra (Fig. 4(b)), the increasing of the Raman shifts and the FWHM of ν_1 mode at 898 cm^{-1} is corresponding to higher vibration energy and low bond stretching mode [19], which will lead to a high $Q \times f$ value. Fig. 6(b) shows the variation in the percentage of lattice energy for each chemical bond as a function of x value. Only the ΣU(Si-O)/U_{cal} shows an increasing trend; therefore, the U_{cal} and $Q \times f$ values become increasingly dependent on the ΣU(Si-O). In fact, the intrinsic loss for microwave dielectric ceramics originates from the anharmonic vibration of the lattice. Changing the bond length, bond strength or lattice energy will affect the $Q \times f$ value.

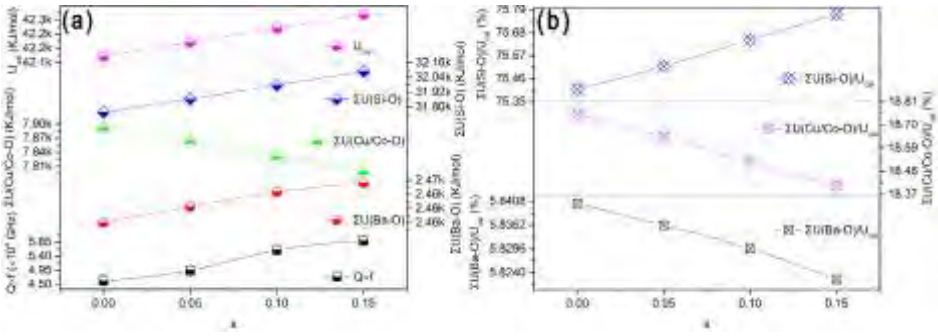

Fig. 6 (a) The $Q\times f$ value, total lattice energy of Ba-O bond, Cu/Co-O bond, Si-O bond and $BaCu_{2-x}Co_xSi_2O_7$ (b) the ratio of Ba-O bond, Cu/Co-O bond and Si-O bond lattice energy to the total lattice energy of $BaCu_{2-x}Co_xSi_2O_7$ (U_{cal}).

Temperature coefficient of resonant frequency (τ_f) represents the temperature stability of resonant frequency and is related to the temperature coefficient of dielectric constant and linear thermal expansion coefficient. The τ_f can be described as follows [40]:

$$\tau_f = -\left(\frac{1}{2}\tau_\varepsilon + \alpha_L\right) \quad (12)$$

where α_L is the linear thermal expansion coefficient, and τ_ε is the temperature coefficient of dielectric constant and represents the temperature stability of dielectric constant. The α_L can be calculated based on the P-V-L theory [46], and the results are shown in Table S4. The linear thermal expansion coefficient of $BaCu_{2-x}Co_xSi_2O_7$ is approximately 6.9 ppm/^{o}C.

Fig. 7 shows the τ_f value and the ratios of the Ba-O, Cu/Co-O and Si-O bond susceptibility to the total susceptibility ($\Sigma\chi^\mu$). The contribution of the susceptibility for each chemical bond is approximately 18% for Ba-O, 41% for Cu/Co-O and 41% for Si-O. The bond susceptibility of $BaCu_{2-x}Co_xSi_2O_7$ is mainly contributed by Cu/Co-O and Si-O bonds. Only the χ(Cu/Co-O)/$\Sigma\chi^\mu$ increases with the x value, and the two other bonds show a downward trend. This result indicates that bond susceptibility starts to become increasingly dependent on Cu/Co-O bond. As shown in Figs. 3(b), 4(b) and 6(a), the variations in the average bond length, Raman shift and lattice energy of Cu/Co-

O bond reveal that the bond stability decreases with increasing *x* value. High Cu/Co-O bond susceptibility and low Cu/Co-O bond stability lead to a drop in the τ_f value.

Table 3 shows the sintering temperature and microwave dielectric properties of some previously reported melilite-type ceramics. The sintering temperature of $BaCu_{2-x}Co_xSi_2O_7$ (x = 0 and 0.15) ceramics is lower than that of other melilite-type ceramics. Furthermore, $BaCu_2Si_2O_7$ ceramics have the smallest $|\tau_f|$ value over other ceramics listed in Table 3.

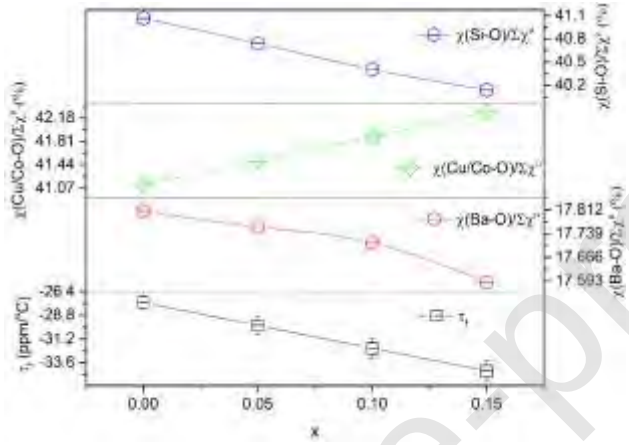

Fig. 7 The τ_f value and the ratio of Ba-O bond, Cu/Co-O bond and Si-O bond susceptibility to the total susceptibility ($\Sigma\chi^{\mu}$).

4. Conclusion

A series of $BaCu_{2-x}Co_xSi_2O_7$ (x = 0-0.15) solid solutions were prepared through the solid state reaction method. Single $BaCu_2Si_2O_7$ phase can be obtained when calcined at 950 ºC for 3 h. However, $BaCuSi_2O_6$ appeared as second phase when the calcining temperature increased to 1075 ºC. The maximum solubility of $BaCu_{2-x}Co_xSi_2O_7$ was located between 0.15 and 0.20. When the Cu^{2+} was replaced by the Co^{2+}, the variation of the cell parameters *a*, *b* and *c* present anisotropic trend. The decreasing of the cell parameters *a* was caused by the stretching of the $[Cu/CoO_4]^{2-}$ chains along the *c* aix. The dielectric constant was dominated by the relative density and ionic polariability. The corrected dielectric constant decreased with the decreasing of ionic polarizability and the total susceptibility ($\Sigma\chi^{\mu}$). The variation of quality factor was highly dependent

on the average bond length and lattice energy, and it increased to the maximum value at x = 0.15. The temperature coefficient of resonant frequency showed a close correlation with the susceptibility of Cu/Co-O bond and the stability of Cu/Co-O bond. With increasing the x value, the average bond length and susceptibility of Cu/Co-O bond increased. Thus, the stability of Cu/Co-O bond decreased and the temperature coefficient of resonant frequency decreased with x value. Optimum microwave dielectric properties were obtained at x = 0.15 when sintered at 1000 ºC for 3 h: ε_r = 8.45, $Q \times f$ = 58958 GHz and τ_f = -34.4 ppm/ºC.

Declaration of interests

The authors declare that they have no known competing financial interests or personal relationships that could have appeared to influence the work reported in this paper.

Acknowledgments

This work was supported by the National Natural Science Foundation of China (NSFC-51572093 and 51772107), Research Project of Electronic Components and Devices of China (1807WM0004), Open Research Fund of State Key Laboratory of Advanced Materials and Electronic Components, Guangdong Fenghua Advanced Technology Holding Co., Ltd. (FHR-JS-201909001), Innovation Team Program of Hubei Province, China (No. 2019CFA004) and the Major Programs of Technical Innovation in Hubei Province of China (2018AAA039). The authors are grateful to the Analytical and Testing Center, Huazhong University of Science and Technology, for SEM analyses.

References

[1] D. Zhou, L.X. Pang, D.W. Wang, C. Li, B.B. Jin, I.M. Reaney, High permittivity and low loss microwave dielectrics suitable for 5G resonators and low temperature co-fired ceramic architecture, J. Mater. Chem. C 5 (2017) 10094-10098.

[2] J. Ren, K. Bi, X. Fu, Z. Peng, Novel Al2Mo3O12-based temperature-stable microwave dielectric ceramics for LTCC applications, J. Mater. Chem. C 6 (2018) 11465-11470.

[3] H. Xiang, C. Li, H. Jantunen, L. Fang, A.E. Hill, Ultralow loss CaMgGeO4 microwave dielectric ceramic and its chemical compatibility with silver electrodes for low-temperature cofired ceramic applications, ACS Sustain. Chem. Eng. 6 (2018) 6458-6466.

[4] D. Zhou, L.X. Pang, D.W. Wang, Z.M. Qi, I.M. Reaney, High quality factor, ultralow sintering temperature Li6B4O9 microwave dielectric ceramics with ultralow density for antenna substrates, ACS Sustain. Chem. Eng. 6 (2018) 11138-11143.

[5] C.F. Xing, B. Wu, J. Bao, H.T. Wu, Y. Zhou, Crystal structure, infrared spectra and microwave dielectric properties of a novel low-firing Gd2Zr3(MoO4)9 ceramic, Ceram. Int. 45 (2019) 22207-22214.

[6] Y.H. Zhang, J.J. Sun, N. Dai, Z.C. Wu, H.T. Wu, C.H. Yang, Crystal structure, infrared spectra and microwave dielectric properties of novel extra low-temperature fired Eu2Zr3(MoO4)9 ceramics, J. Eur. Ceram. Soc. 39 (2019) 1127-1131.

[7] Z.Y. Zou, Z.H. Chen, X.K. Lan, W.Z. Lu, B. Ullah, X.H. Wang, W. Lei, Weak ferroelectricity and low-permittivity microwave dielectric properties of Ba2Zn(1+x)Si2O(7+x) ceramics, J. Eur. Ceram. Soc. 37 (2017) 3065-3071.

[8] R.D. Adams, C. Payen, T. Datta, Syntheses, structural analyses, and unusual magnetic properties of Ba2CoSi2O7 and BaCo2Si2O7, Inorg. Chem. 35 (1996) 3492-3497.

[9] C. Thieme, T. Waurischk, S. Heitmann, C. Rüssel, New family of materials with negative coefficients of thermal expansion: the effect of MgO, CoO, MnO, NiO, or CuO

on the phase stability and thermal expansion of solid solution phases derived from BaZn2Si2O7, Inorg. Chem. 55 (2016) 4476-4484.

[10] T. Joseph, M.T. Sebastian, Microwave dielectric properties of (Sr1-xAx)2(Zn1-xBx)Si2O7 ceramics (A = Ca, Ba and B = Co, Mg, Mn, Ni), J. Am. Ceram. Soc. 93 (2010) 147-154.

[11] M. Xiao, Y. Wei, P. Zhang, The correlations between complex chemical bond theory and microwave dielectric properties of Ca2MgSi2O7 ceramics, J. Electron. Mater. 48 (2019) 1652-1659.

[12] M. Xiao, Y. Wei, H. Sun, J. Lou, P. Zhang, Crystal structure and microwave dielectric properties of low-permittivity Sr2MgSi2O7 ceramic, J. Mater. Sci-Mater. El. 29 (2018) 20339-20346.

[13] C. Li, C. Yin, J. Chen, H. Xiang, Y. Tang, L. Fang, Crystal structure and dielectric properties of germanate melilites Ba2MGe2O7 (M = Mg and Zn) with low permittivity, J. Eur. Ceram. Soc. 38 (2018) 5246-5251.

[14] G.H. Wang, C.Y. Xu, H.B. Cao, T. Hong, Q. Huang, Q.Y. Ren, J. Ma, Magnetic properties of the low-dimensional BaM2Si2O7 system (M = Cu, Co, Mn), Phys. Rev. B 100 (2019) 035131.

[15] H.M. Rietveld, A profile refinement method for nuclear and magnetic structures, J. Appl. Cryst. 2 (1969) 65-71.

[16] A.C. Larson, R.B. Dreele, General structure analysis system (GSAS), Los Alamos National Laboratory Report LAUR 1994 86-748.

[17] B.H. Toby, EXPGUI, a graphical user interface for GSAS, J. Appl. Cryst. 34 (2001) 210-213.

[18] B.W. Hakki, P.D. Coleman, A dielectric resonator method of measuring inductive capacities in the millimeter range, IRE Trans. Microwave Theory Technol. 8 (1960) 402-410.

[19] X.Q. Song, M.Q. Xie, K. Du, W.Z. Lu, W. Lei, Synthesis, crystal structure and microwave dielectric properties of self-temperature stable Ba1-xSrxCuSi2O6 ceramics for millimeter-wave communication, Journal of Materiomics 5 (2019), 606-617.

[20]R.D. Shannon, Revised effective ionic radii and systematic studies of interatomic distances in halides and chalcogenides, Acta Crystallogr. Sect. A 32 (1976), 751-767.

[21]M. Kerstan, M. Müller, C. Rüssel, Thermal expansion of Ba2ZnSi2O7, BaZnSiO4 and the solid solution series BaZn2-xMgxSi2O7 ($0 \leq x \leq 2$) studied by high-temperature X-ray diffraction and dilatometry, J. Solid State Chem. 188 (2012) 84-91.

[22]H. Yang, R.T. Downs, S.H. Evans, W.W. Pinch, Scottyite, the natural analog of synthetic BaCu2Si2O7, a new mineral from the Wessels mine, Kalahari Manganese Fields, South Africa, Am. Mineral. 98 (2013), 478-484.

[23]Y. Xia, Q. Ma, Z. Zhang, Z. Liu, J. Feng, A. Shao, Q. Fu, Development of Chinese barium copper silicate pigments during the Qin Empire based on Raman and polarized light microscopy studies, J. Archaeol. Sci. 49 (2014) 500-509.

[24]Q. Liao, L. Li, Structural dependence of microwave dielectric properties of ixiolite structured ZnTiNb2O8 materials: crystal structure refinement and Raman spectra study, Dalton T. 41 (2012) 6963-6969.

[25]H.J. Jo, E.S. Kim, Effect of Sn4+ substitution on microwave dielectric properties of (Mg0.95Ni0.05)(Ti1-xSnx)O3 ceramics, Mater. Res. Bull. 67 (2015) 221-225.

[26]S.J. Webb, J. Breeze, R.I. Scott, D.S. Cannell, D.M. Iddles, N.M. Alford, Raman spectroscopic study of gallium-doped Ba(Zn1/3Ta2/3)O3, J. Am. Ceram. Soc. 85 (2002) 1753-1756.

[27]Y. Lai, H. Su, G. Wang, X. Tang, X. Huang, X. Liang, X.R. Wang, Low-temperature sintering of microwave ceramics with high Qf values through LiF addition, J. Am. Ceram. Soc. 102 (2019), 1893-1903.

[28]C. Diao, F. Shi, Correlation among dielectric properties, vibrational modes, and crystal structures in Ba[SnxZn(1–x)/3Nb2(1–x)/3]O3 solid solutions, J. Phys. Chem. C 116 (2012) 6852-6858.

[29]S.J. Penn, N.M. Alford, A. Templeton, X. Wang, M. Xu, M. Reece, K. Schrapel, Effect of porosity and grain size on the microwave dielectric properties of sintered alumina, J. Am. Ceram. Soc. 80 (1997) 1885-1888.

[30]H. Tamura, Microwave dielectric losses caused by lattice defects, J. Eur. Ceram.

Soc. 26 (2006) 1775-1780.

[31] J.C. Phillips, Dielectric definition of electronegativity, Phys. Rev. Lett. 20 (1968) 550-553.

[32] J.C. Phillips, J.A. Van Vechten, Dielectric classification of crystal structures, ionization potentials, and band structures, Phys. Rev. Lett. 22 (1969) 705-708.

[33] J.A. Van Vechten, Quantum dielectric theory of electronegativity in covalent systems. I. Electronic dielectric constant, Phys. Rev. 182 (1969) 891-905.

[34] J.C. Phillips, Ionicity of the chemical bond in crystals, Rev. Mod. Phy. 42 (1970) 317-356.

[35] B.F. Levine, Bond susceptibilities and ionicities in complex crystal structures, J. Chem. Phys. 59 (1973) 1463-1486.

[36] B.F. Levine, Bond-charge calculation of nonlinear optical susceptibilities for various crystal structures, Phys. Rev. B 7 (1973) 2600-2626.

[37] Z.J. Wu, S.Y. Zhang, Semiempirical method for the evaluation of bond covalency in complex crystals, J. Chem. Phys. A 103 (1999) 4270-4274.

[38] B. Zhang, L. Li, Investigation of chemical bonds in the ordered Ba3Zn(Nb2-xMox)O9+x/2 ceramics and its effects on the microwave performance, J. Eur. Ceram. Soc. 38 (2018) 4446-4452.

[39] D. Xue, S. Zhang, Calculation of the nonlinear optical coefficient of the crystal, J. Phys-Condens. Mat. 8 (1996), 1949-1956.

[40] A.J. Bosman, E.E. Havinga, Temperature dependence of dielectric constants of cubic ionic compounds, Phys. Rev. 129 (1963) 1593.

[41] Q. Lin, K. Song, B. Liu, H.B. Bafrooei, D. Zhou, W. Su, I.M. Reaney, Vibrational spectroscopy and microwave dielectric properties of AY2Si3O10 (A = Sr, Ba) ceramics for 5 G applications, Ceram. Int. 46 (2019) 1171-1177.

[42] H. Xiang, L. Fang, W. Fang, Y. Tang, C. Li, A novel low-firing microwave dielectric ceramic Li2ZnGe3O8 with cubic spinel structure, J. Eur. Ceram. Soc. 37 (1017) 625-629.

[43] E.S. Kim, B.S. Chun, R. Freer, R.J. Cernik, Effects of packing fraction and bond

valence on microwave dielectric properties of A2+B6+O4 (A2+: Ca, Pb, Ba; B6+: Mo, W) ceramics, J. Eur. Ceram. Soc. 30 (2010), 1731-1736.

[44] W.S. Xia, L.X. Li, P.F. Ning, Q.W. Liao, Relationship between bond ionicity, lattice energy, and microwave dielectric properties of Zn(Ta1-xNbx)2O6 ceramics, J. Am. Ceram. Soc. 95 (2012) 2587-2592.

[45] H. Yang, S. Zhang, H. Yang, X. Zhang, E. Li, Structural evolution and microwave dielectric properties of xZn0.5Ti0.5NbO4-(1-x)Zn0.15Nb0.3Ti0.55O2 ceramics, Inorg. Chem. 57 (2018) 8264-8275.

[46] H. Yang, S. Zhang, Y. Chen, H. Yang, Y. Yuan, E. Li, Crystal chemistry, Raman spectra, and bond characteristics of trirutile-type Co0.5Ti0.5TaO4 microwave dielectric ceramics, Inorg. Chem. 58 (2018) 968-976.

[47] C. Yin, Y. Tang, J. Chen, F. Li, Y. Huang, C. Li, L. Fang, (2019). Two low-permittivity melilite ceramics in the SrO-MO-GeO2 (M = Mg, Zn) system and their temperature stability through compositional modifications, J. Eur. Ceram. Soc. 40 (2019) 1186-1190.

[48] X.Q. Song, W. Lei, M.Q. Xie, J. Li, X.C. Wang, W.Z. Lu, Sintering behaviour, lattice energy and microwave dielectric properties of melilite-type BaCo2Si2O7 ceramics, Mater. Res. Express 6 (2019) 126322.

Table 1 Lattice parameters, density and Rietveld discrepancy factors of $BaCu_{2-x}Co_xSi_2O_7$ ceramics.

x	a (Å)	b (Å)	c (Å)	V (Å^3)	ρ_{bul} (g/cm^3)	ρ_{the} (g/cm^3)	ρ_{rel} (%)	Rp	Rwp	χ^2
0	6.8601(1)	13.1744(1)	6.8968(1)	623.31(1)	4.468	4.610	96.920	0.0453	0.0352	3.874
0.05	6.8575(1)	13.1786(1)	6.8994(1)	623.51(1)	4.521	4.606	98.144	0.0451	0.0332	3.482
0.10	6.8565(1)	13.1839(1)	6.9051(1)	624.19(1)	4.540	4.598	98.743	0.0439	0.0325	3.162
0.15	6.8537(1)	13.1862(2)	6.9089(1)	624.39(2)	4.558	4.587	99.370	0.0469	0.0329	3.472

Table 2 Microwave dielectric properties of $BaCu_{2-x}Co_xSi_2O_7$ ceramics sintered at their optimum temperature for 3 h.

x	S.T. (°C)	ε_r ($\varepsilon_{r\text{-mea}}$)	$\varepsilon_{r\text{-cal}}$	$\varepsilon_{r\text{-corr}}$	Qf (GHz)	τ_f (ppm/°C)
0	1025	8.29 ± 0.03	8.36	8.67	46085 ± 2100	-27.5 ± 0.7
0.05	1025	8.35 ± 0.02	8.33	8.58	49487 ± 1900	-29.8 ± 0.9
0.10	1025	8.40 ± 0.03	8.28	8.56	55968 ± 1700	-32.1 ± 1.0
0.15	1000	8.45 ± 0.02	8.25	8.53	58958 ± 1600	-34.4 ± 1.1

S.T.: Sintering temperature.

Table 3 Sintering temperature and microwave dielectric properties of some melilite-type ceramics.

Compounds	S.T. (°C)	ε_r	Qf (GHz)	τ_f (ppm/°C)	Reference
$Sr_2ZnSi_2O_7$	1475	8.40	105000	-51.5	10
$Sr_2CoSi_2O_7$	1375	8.90	34000	-56.7	
$Sr_2MnSi_2O_7$	1375	8.80	32000	-58.8	
$Ca_2ZnSi_2O_7$	1300	11.00	13500	-64.3	
$Ca_2MgSi_2O_7$	1300	9.86	8016	-42.0	11
$Sr_2MgSi_2O_7$	1280	6.85	22530	-32.0	12
$Ba_2MgGe_2O_7$	1280	7.76	20700	-55.0	13
$Ba_2ZnGe_2O_7$	1180	9.00	13950	-75	
$Sr_2MgGe_2O_7$	1330	8.56	28800	-70.5	47
$Sr_2ZnGe_2O_7$	1290	8.81	35700	-84.4	
$BaCo_2Si_2O_7$	1060	9.26	31135	-92.1	48
$BaCu_2Si_2O_7$	1025	8.29	46085	-27.5	This work
$BaCu_{1.85}Co_{0.15}Si_2O_7$	1000	8.45	58958	-34.4	

S.T.: Sintering temperature.